Stabilization parameter analysis of a second-order linear numerical scheme for the nonlocal Cahn–Hilliard equation

Xiao Li and Zhonghua Qiao*

*Department of Applied Mathematics, The Hong Kong Polytechnic University,
Hung Hom, Kowloon, Hong Kong*
*Corresponding author: zqiao@polyu.edu.hk

AND

Cheng Wang

Department of Mathematics, The University of Massachusetts, North Dartmouth, MA 02747, USA

A second-order accurate (in time) and linear numerical scheme is proposed and analyzed for the nonlocal Cahn–Hilliard equation. The backward differentiation formula is used as the temporal discretization, while an explicit extrapolation is applied to the nonlinear term and the concave expansive term. In addition, an $O(\Delta t^2)$ artificial regularization term, in the form of $A\Delta_N(\phi^{n+1} - 2\phi^n + \phi^{n-1})$, is added for the sake of numerical stability. The resulting constant-coefficient linear scheme brings great numerical convenience; however, its theoretical analysis turns out to be very challenging, due to the lack of higher-order diffusion in the nonlocal model. In fact, a rough energy stability analysis can be derived, where an assumption on the ℓ^∞ bound of the numerical solution is required. To recover such an ℓ^∞ bound, an optimal rate convergence analysis has to be conducted, which combines a high-order consistency analysis for the numerical system and the stability estimate for the error function. We adopt a novel test function for the error equation, so that a higher-order temporal truncation error is derived to match the accuracy for discretizing the temporal derivative. Under the view that the numerical solution is actually a small perturbation of the exact solution, a uniform ℓ^∞ bound of the numerical solution can be obtained, by resorting to the error estimate under a moderate constraint of the time step size. Therefore, the result of the energy stability is restated with a new assumption on the stabilization parameter A. Some numerical experiments are carried out to display the behavior of the proposed second-order scheme, including the convergence tests and long-time coarsening dynamics.

Keywords: nonlocal Cahn–Hilliard equation; second-order accurate scheme; higher-order consistency analysis; rough error estimate and refined error estimate; energy stability.

1. Introduction

The nonlocal Cahn–Hilliard (NCH) equation is taken into consideration, which turns out to be the H^{-1} gradient flow with respect to the free energy functional with nonlocal interaction effect as follows (Bates & Han, 2005a,b; Bates, 2006; Bates *et al.*, 2006; Bates *et al.*, 2009; Guan *et al.*, 2017, 2014a,b):

$$E(\phi) = \int_\Omega \left(\frac{1}{4}\phi^4 - \frac{1}{2}\phi^2 + \frac{\varepsilon^2}{4}\int_\Omega J(\mathbf{x} - \mathbf{y})(\phi(\mathbf{x}) - \phi(\mathbf{y}))^2 \, d\mathbf{y} \right) d\mathbf{x}, \qquad (1.1)$$

where $\varepsilon > 0$ is an interfacial parameter and $\Omega = \prod_{i=1}^d (-X_i, X_i)$ is a rectangular domain in $\mathbb{R}^d$. The kernel function J is required to satisfy the following conditions (Du *et al.*, 2018; Li *et al.*, 2021):

(a) $J(\mathbf{x}) \geqslant 0$ for any $\mathbf{x} \in \Omega$, and $\int_\Omega J(\mathbf{x})\,\mathrm{d}\mathbf{x} > 0$;

(b) J is Ω-periodic and even, i.e., $J(-\mathbf{x}) = J(\mathbf{x})$ for any $\mathbf{x} \in \mathbb{R}^d$;

(c) $\frac{1}{2} \int_\Omega J(\mathbf{x})|\mathbf{x}|^2\,\mathrm{d}\mathbf{x} = 1$,

where condition (c) means that J has a finite second moment in Ω. A nonlocal linear operator is introduced as $\mathscr{L} : \psi(\mathbf{x}) \mapsto \int_\Omega J(\mathbf{x} - \mathbf{y})(\psi(\mathbf{x}) - \psi(\mathbf{y}))\,\mathrm{d}\mathbf{y}$. Then, using condition (a), it is clear that $\mathscr{L}\psi = (J * 1)\psi - J * \psi$ with the following periodic convolution (Guan *et al.*, 2014b):

$$(J * \psi)(\mathbf{x}) = \int_\Omega J(\mathbf{x} - \mathbf{y})\psi(\mathbf{y})\,\mathrm{d}\mathbf{y} = \int_\Omega J(\mathbf{y})\psi(\mathbf{x} - \mathbf{y})\,\mathrm{d}\mathbf{y}.$$

By condition (c), a careful calculation yields an equivalent form of the energy (1.1) as

$$E(\phi) = \int_\Omega F(\phi)\,\mathrm{d}\mathbf{x} + \frac{\varepsilon^2}{2}(\mathscr{L}\phi, \phi)_{L^2}, \quad \text{with } F(\phi) = \frac{1}{4}\phi^4 - \frac{1}{2}\phi^2, \tag{1.2}$$

and the chemical potential becomes

$$\mu := \delta_\phi E(\phi) = \phi^3 - \phi + \varepsilon^2 \mathscr{L}\phi.$$

As a consequence, the corresponding NCH equation turns out to be

$$\partial_t \phi = \Delta\mu = \Delta(\phi^3 - \phi + \varepsilon^2 \mathscr{L}\phi) = \Delta[\phi^3 - \phi + \varepsilon^2((J * 1)\phi - J * \phi)], \tag{1.3}$$

subject to the periodic boundary condition. The mass conservation of ϕ is obvious in the sense that $\frac{\mathrm{d}}{\mathrm{d}t} \int_\Omega \phi(\mathbf{x}, t)\,\mathrm{d}\mathbf{x} = 0$. In addition, the following diffusivity condition is taken:

$$\gamma_0 := \varepsilon^2(J * 1) - 1 > 0. \tag{1.4}$$

Without such a condition, the solution may exhibit some singular behaviors.

As a nonlocal variant of the classic Cahn–Hilliard equation (Cahn & Hilliard, 1958), the NCH equation has increasingly attracted attention and been widely used in various areas ranging from chemistry, material science to finance and image processing. The well-posedness of the NCH equation (1.3) equipped with Neumann or Dirichlet boundary condition was studied in Bates & Han (2005a,b), and it was pointed out in Guan *et al.* (2014b) that the existence and uniqueness of the solution to the NCH equation subject to the periodic boundary condition may also be established by using a similar technique. A brief review of some parabolic-like evolution equations was made in Fife (2003), including nonlocal and pattern-formation problems, along with a comparison between the local and nonlocal equations.

Numerical investigations of nonlocal models have also attracted much attention in recent years. For a family of nonlocal diffusion equations equipped with various boundary conditions, finite difference, finite element and spectral approximations were discussed in Zhou & Du (2010), Tian & Du (2014), Du *et al.* (2018) and Du *et al.* (2019b). Bates *et al.* (2006, 2009) studied ℓ^∞ stable and convergent numerical schemes for the nonlocal Allen–Cahn equation and related equation. An exponential time differencing method was applied to the nonlocal Allen–Cahn equation to establish first- and second-order accurate, ℓ^∞ stable linear numerical schemes in Du *et al.* (2019a), and further extended to a class of semilinear parabolic equations in Du *et al.* (2021). In particular, the energy stability (induced by the energetic variational formulation) has played a very important role in the numerical approximations. A theoretical justification of energy stability has been provided for a few first-order numerical schemes (Guan *et al.*, 2014b; Li *et al.*, 2021), based on the convex splitting and linearized stabilization ideas, respectively. For the second-order numerical schemes, the only existing energy stability and convergence analysis

has been reported for a higher-order convex splitting method (Guan *et al.*, 2014a, 2017). Meanwhile, the computational cost for such a numerical approach turns out to be expensive, because of an implicit treatment for the nonlinear term (to ensure the energy stability).

Consequently, a second-order accurate, linear and energy stable numerical scheme is highly desired for the NCH equation. In fact, this effort has been successful for the classic Cahn–Hilliard model (Li & Qiao, 2017a,b), in which a stabilization term is added in the numerical scheme and a modified energy stability is theoretically established. However, these works rely heavily on the higher-order surface diffusion term in the classic Cahn–Hilliard model, so that the reported methodology is hardly applicable to the NCH model. In this paper, we propose and analyze a second-order accurate and linear numerical scheme for the NCH equation, with the energy stability and convergence analysis theoretically justified. In more details, the second-order backward differentiation formula (BDF2) is chosen as the temporal discretization, combined with an implicit treatment of the nonlocal term, as well as explicit extrapolation for the nonlinear term and concave expansive term. Moreover, an $O(\Delta t^2)$ artificial stabilization term is added in the form of $A\Delta_N(\phi^{n+1} - 2\phi^n + \phi^{n-1})$. In turn, this numerical scheme can be solved by using the fast Fourier transform, so that the nonlocal term does not cause much computation in comparison with the Laplacian term in the classic Cahn–Hilliard equation. To establish the energy stability, a uniform ℓ^∞ bound of the numerical solution is assumed and the requirement for the stabilizing constant turns out to depend on the unknown numerical solution. Subsequently, we conduct a novel convergence analysis of the proposed stabilized BDF2 scheme to recover such a requirement, by applying the high-order consistency analysis, so that the uniform ℓ^∞ bound of the numerical solution can be theoretically justified. A crucial difference with the standard error estimate is that we adopt $(-\Delta_N)^{-1}(\hat{e}^{n+1} - \hat{e}^n)$ to test the error equation with respect to the numerical error function $\hat{e}^n$, instead of testing $(-\Delta_N)^{-1}\hat{e}^{n+1}$ as in a recent work (Li *et al.*, 2021) for the first-order scheme (where $(-\Delta_N)^{-1}$ is a spatial discrete operator to be defined in the next section). In other words, the key point is to use the discrete temporal derivative of the error function as the test function, rather than the error function directly, which would provide a higher-order temporal truncation error to match the BDF2 discretization for the temporal derivative. Resorting to the convergence result, we obtain a uniform ℓ^∞ bound of the numerical solution by viewing it as a perturbation of the exact solution. As a result, the *a priori* assumption is recovered and a new condition is derived for the stabilizing constant in the energy stability analysis.

The rest of the paper is organized as follows. In Section 2, the stabilized BDF2 scheme is presented in the fully discrete form and an energy stability is established with respect to a modified energy under an assumption of the uniform ℓ^∞ bound of the numerical solution. Convergence analysis is presented in Section 3, which is the main part of the paper, including the high-order consistency analysis, a rough error estimate based on the stability analysis and a refined error estimate based on *a priori* bound obtained by the rough estimate. Consequently, the uniform ℓ^∞ bound of the numerical solution is recovered and the energy stability result is restated under a new requirement on the stabilizing constant. In Section 4, some numerical experiments are carried out to display the behavior of the proposed numerical scheme. Finally, some concluding remarks are given in Section 5.

2. The numerical scheme and energy stability analysis

2.1 *The Fourier pseudo-spectral spatial discretization*

We adopt the two-dimensional Fourier pseudo-spectral method. An extension to the three-dimensional spatial discretization is straightforward. To simplify the notations in the later analysis, we assume that the domain is given by $\Omega = (-1, 1)^2$ and denote by $C_{\text{per}}^m(\Omega)$ the set of all C^m-functions with period 2,

along each coordinate direction. Let N be an even number: $N = 2K$ for some $K \in \mathbb{N}$; the analyses for more general cases are a bit more tedious, but can be carried out without essential difficulty. The spatial variables are evaluated on the standard two-dimensional numerical grid Ω_N, which is defined by grid points (x_i, y_j) with $x_i = -1 + ih$, $y_j = -1 + jh$, $0 \leqslant i,j \leqslant N$ and $h = 2/N = 1/K$.

The grid function space is defined as

$$\mathscr{M}_h := \{f : \mathbb{Z}^2 \to \mathbb{R} \,|\, f \text{ is } \Omega_N \text{-periodic}\}.$$

For any grid functions $f, g \in \mathscr{M}_h$, the ℓ^2 inner product and norm are defined as

$$\langle f, g \rangle := h^2 \sum_{i,j=0}^{N-1} f_{i,j} \cdot g_{i,j}, \quad \|f\|_2 := \sqrt{\langle f, f \rangle}.$$

The zero-mean grid function subspace is denoted as $\mathscr{M}_h^0 := \{f \in \mathscr{M}_h \,|\, \bar{f} = 0\}$ with $\bar{f} := \frac{1}{4}\langle f, 1 \rangle$. For $f \in \mathscr{M}_h$, we have the discrete Fourier expansion

$$f_{i,j} = \sum_{\ell,m=-K+1}^{K} \hat{f}_{\ell,m}^N \exp(\pi \mathrm{i}(\ell x_i + m y_j)), \quad \hat{f}_{\ell,m}^N := \frac{1}{N^2} \sum_{i,j=0}^{N-1} f_{i,j} \exp(-\pi \mathrm{i}(\ell x_i + m y_j)).$$

The Fourier pseudo-spectral first- and second-order derivatives of f are defined as

$$\mathscr{D}_x f_{i,j} := \sum_{\ell,m=-K+1}^{K} (\pi \mathrm{i}\ell)\hat{f}_{\ell,m}^N \exp(\pi \mathrm{i}(\ell x_i + m y_j)),$$

$$\mathscr{D}_x^2 f_{i,j} := \sum_{\ell,m=-K+1}^{K} (-\pi^2 \ell^2)\hat{f}_{\ell,m}^N \exp(\pi \mathrm{i}(\ell x_i + m y_j)).$$

The differentiation operators in the y direction, $\mathscr{D}_y$ and $\mathscr{D}_y^2$, can be defined in the same fashion. In turn, for any $f \in \mathscr{M}_h$ and $\boldsymbol{f} = (f^1, f^2) \in \mathscr{M}_h \times \mathscr{M}_h$, the discrete gradient, divergence and Laplacian operators are given respectively by

$$\nabla_N f = \begin{pmatrix} \mathscr{D}_x f \\ \mathscr{D}_y f \end{pmatrix}, \qquad \nabla_N \cdot \boldsymbol{f} = \mathscr{D}_x f^1 + \mathscr{D}_y f^2, \qquad \Delta_N f = \mathscr{D}_x^2 f + \mathscr{D}_y^2 f.$$

Moreover, the following summation-by-parts formulas are valid (Gottlieb *et al.*, 2012; Gottlieb & Wang, 2012; Cheng *et al.*, 2016; Li *et al.*, 2021): for any periodic grid functions $f, g \in \mathscr{M}_h$ and $\boldsymbol{g} \in \mathscr{M}_h \times \mathscr{M}_h$,

$$\langle f, \nabla_N \cdot \boldsymbol{g} \rangle = -\langle \nabla_N f, \boldsymbol{g} \rangle, \qquad \langle f, \Delta_N g \rangle = -\langle \nabla_N f, \nabla_N g \rangle = \langle \Delta_N f, g \rangle.$$

In addition, $-\Delta_N$ is self-adjoint and positive definite, and thus invertible, on $\mathscr{M}_h^0$.

Since the NCH equation (1.3) is an H^{-1} gradient flow of (1.2), we need a discrete version of the H^{-1} norm defined on $\mathcal{M}_h^0$. For any $f, g \in \mathcal{M}_h^0$, we define

$$\langle f, g \rangle_{-1,N} := \langle f, (-\Delta_N)^{-1} g \rangle = \langle (-\Delta_N)^{-\frac{1}{2}} f, (-\Delta_N)^{-\frac{1}{2}} g \rangle,$$

then the discrete H_h^{-1} norm $\| \cdot \|_{-1,N}$ can be introduced as

$$\|f\|_{-1,N} := \sqrt{\langle f, f \rangle_{-1,N}} = \|(-\Delta_N)^{-\frac{1}{2}} f\|_2, \quad f \in \mathcal{M}_h^0.$$

In addition to the standard ℓ^2 norm, we also introduce the ℓ^p, $1 \leqslant p < \infty$ and ℓ^∞ norms for a grid function $f \in \mathcal{M}_h$:

$$\|f\|_\infty := \max_{i,j} |f_{i,j}|, \qquad \|f\|_p := \left(h^2 \sum_{i,j=0}^{N-1} |f_{i,j}|^p \right)^{\frac{1}{p}}, \quad 1 \leq p < \infty.$$

The definition of the discrete convolution follows similar notations in Guan *et al.* (2014b) and Li *et al.* (2021). For any $\psi, f \in \mathcal{M}_h$, the discrete convolution $\psi \circledast f \in \mathcal{M}_h$ is introduced at a component-wise level:

$$(\psi \circledast f)_{ij} = h^2 \sum_{m,n=0}^{N-1} \psi_{i-m,j-n} f_{mn}, \qquad 0 \leqslant i, j \leqslant N-1.$$

In addition, the following preliminary estimate is needed in the convergence analysis; the detailed proof has been provided in a recent work (Li *et al.*, 2021), and the finite difference version has been analyzed in Guan *et al.* (2014b).

LEMMA 2.1 (Li *et al.*, 2021) Suppose $\mathsf{J} \in C^1_{\text{per}}(\Omega)$ and define its grid restriction by $J_{ij} := \mathsf{J}(x_i, y_j)$. Then for any $\phi, \psi \in \mathcal{M}_h$ and any $\alpha > 0$, we have

$$|\langle J \circledast \phi, \Delta_N \psi \rangle| \leqslant \alpha \|\phi\|_2^2 + \frac{C_\mathsf{J}}{\alpha} \|\nabla_N \psi\|_2^2,$$

where C_J is a positive constant depending on J and Ω, but independent of h.

Given a kernel J satisfying conditions (a)–(c), the discrete version of the nonlocal operator $\mathscr{L}$ can be represented as

$$\mathscr{L}_N f = (J \circledast 1) f - J \circledast f, \quad f \in \mathcal{M}_h.$$

It is easy to verify that $\mathscr{L}_N$ commutes with Δ_N, and is self-adjoint and positive semi-definite. Meanwhile, the discrete version of the energy (1.2) is introduced as

$$E_N(v) = \langle F(v), 1 \rangle + \frac{\varepsilon^2}{2} \langle \mathscr{L}_N v, v \rangle, \quad v \in \mathcal{M}_h.$$

For the sake of brevity, we use $*$, instead of $\circledast$, to denote the discrete convolutions below and the meaning depends on the functions on both sides of the notation.

2.2 *The fully discrete scheme and energy stability analysis*

Set Δt as a uniform time step size and $\{t_k = k\Delta t\}$ as the sequence of discrete time instants. Denote ϕ^k ($k \geqslant 0$) as the numerical solution of the phase variable at time step t_k. The stabilized BDF2 scheme is proposed as follows: given $\phi^n, \phi^{n-1} \in \mathscr{M}_h^0$, find $\phi^{n+1} \in \mathscr{M}_h^0$ such that

$$\frac{\frac{3}{2}\phi^{n+1} - 2\phi^n + \frac{1}{2}\phi^{n-1}}{\Delta t} = \Delta_N\Big((\check{\phi}^{n+1})^3 - \check{\phi}^{n+1} + A(\phi^{n+1} - 2\phi^n + \phi^{n-1}) + \varepsilon^2 \mathscr{L}_N\phi^{n+1}\Big), \quad (2.1)$$

where $\check{\phi}^{n+1} = 2\phi^n - \phi^{n-1}$.

Since the proposed numerical scheme (2.1) is a two-step algorithm, an accurate approximation for the phase variable value at t_1 is needed in the initialization process. It is well known that a single-step numerical method would create a numerical solution with higher-order temporal accuracy (than the order of truncation error) in the first step, if the exact initial data is imposed. Also, see the detailed analysis in the related works (Guo *et al.*, 2016, 2021) for local Cahn–Hilliard equation, in which a single-step, first-order semi-implicit algorithm creates a second-order accurate numerical solution in the first step. For the NCH equation, a higher-order approximation at time step t_1 is more preferred, to facilitate the higher-order asymptotic consistency analysis presented in the later sections. For example, the second-order Runge–Kutta (RK2) method could be applied in the first step, which in turn gives an $O(\Delta t^3 + h^m)$ approximation at t_1, if an exact initial data is imposed.

We have the following result on the energy stability with respect to a modified energy.

PROPOSITION 2.2   For the stabilized BDF2 scheme (2.1), a modified energy dissipation property is available:

$$\tilde{E}_N(\phi^{n+1}, \phi^n) \leqslant \tilde{E}_N(\phi^n, \phi^{n-1}), \quad (2.2)$$

where

$$\tilde{E}_N(\phi^{n+1}, \phi^n) := E_N(\phi^{n+1}) + \frac{A+1}{2}\|\phi^{n+1} - \phi^n\|_2^2 + \frac{1}{4\Delta t}\|\phi^{n+1} - \phi^n\|_{-1,N}^2,$$

if the following constraints are valid with C_J dependent only on the kernel J and Ω:

$$A \geqslant \frac{9}{2\gamma_0}(\|2\phi^n - \phi^{n-1}\|_\infty^2 + \|\phi^{n+1}\|_\infty^2)^2 - 1, \quad C_J\varepsilon^4\Delta t \leqslant \gamma_0. \quad (2.3)$$

Proof.   Taking a discrete inner product with (2.1) by $(-\Delta_N)^{-1}(\phi^{n+1} - \phi^n)$ gives

$$\frac{1}{\Delta t}\Big\langle \frac{3}{2}\phi^{n+1} - 2\phi^n + \frac{1}{2}\phi^{n-1}, \phi^{n+1} - \phi^n\Big\rangle_{-1,N} + A\langle\phi^{n+1} - 2\phi^n + \phi^{n-1}, \phi^{n+1} - \phi^n\rangle$$

$$= -\langle(\check{\phi}^{n+1})^3, \phi^{n+1} - \phi^n\rangle + \langle\check{\phi}^{n+1}, \phi^{n+1} - \phi^n\rangle - \varepsilon^2\langle\mathscr{L}_N\phi^{n+1}, \phi^{n+1} - \phi^n\rangle, \quad (2.4)$$

in which summation-by-parts formulas have been repeatedly applied.

For the left-hand side term associated with the temporal stencil, the following estimate is straightforward:

$$
\begin{aligned}
\left\langle \frac{3}{2}\phi^{n+1} - 2\phi^n + \frac{1}{2}\phi^{n-1}, \phi^{n+1} - \phi^n \right\rangle_{-1,N} & \\
&= \left\langle \frac{3}{2}(\phi^{n+1} - \phi^n) - \frac{1}{2}(\phi^n - \phi^{n-1}), \phi^{n+1} - \phi^n \right\rangle_{-1,N} \\
&\geqslant \frac{3}{2}\|\phi^{n+1} - \phi^n\|_{-1,N}^2 - \frac{1}{4}(\|\phi^{n+1} - \phi^n\|_{-1,N}^2 + \|\phi^n - \phi^{n-1}\|_{-1,N}^2) \\
&= \frac{5}{4}\|\phi^{n+1} - \phi^n\|_{-1,N}^2 - \frac{1}{4}\|\phi^n - \phi^{n-1}\|_{-1,N}^2.
\end{aligned}
\tag{2.5}
$$

For the artificial regularization term, the following identity is valid:

$$
\langle \phi^{n+1} - 2\phi^n + \phi^{n-1}, \phi^{n+1} - \phi^n \rangle = \frac{1}{2}(\|\phi^{n+1} - \phi^n\|_2^2 - \|\phi^n - \phi^{n-1}\|_2^2 + \|\phi^{n+1} - 2\phi^n + \phi^{n-1}\|_2^2).
\tag{2.6}
$$

For the second linear term on the right-hand side, noticing that

$$
\check{\phi}^{n+1} = \phi^{n+1} - (\phi^{n+1} - 2\phi^n + \phi^{n-1}),
\tag{2.7}
$$

we have

$$
\begin{aligned}
\langle \check{\phi}^{n+1}, \phi^{n+1} - \phi^n \rangle &= \langle \phi^{n+1}, \phi^{n+1} - \phi^n \rangle - \langle \phi^{n+1} - 2\phi^n + \phi^{n-1}, \phi^{n+1} - \phi^n \rangle \\
&= \frac{1}{2}(\|\phi^{n+1}\|_2^2 - \|\phi^n\|_2^2 + \|\phi^{n+1} - \phi^n\|_2^2) \\
&\quad - \frac{1}{2}(\|\phi^{n+1} - \phi^n\|_2^2 - \|\phi^n - \phi^{n-1}\|_2^2 + \|\phi^{n+1} - 2\phi^n + \phi^{n-1}\|_2^2).
\end{aligned}
\tag{2.8}
$$

The nonlocal diffusion term on the right-hand side can be rewritten as follows:

$$
\begin{aligned}
\varepsilon^2 \langle \mathscr{L}_N \phi^{n+1}, \phi^{n+1} - \phi^n \rangle &= \frac{\varepsilon^2}{2}(\langle \mathscr{L}_N \phi^{n+1}, \phi^{n+1} \rangle - \langle \mathscr{L}_N \phi^n, \phi^n \rangle) \\
&\quad + \frac{\varepsilon^2}{2}(J * 1)\|\phi^{n+1} - \phi^n\|_2^2 - \frac{\varepsilon^2}{2}\langle J * (\phi^{n+1} - \phi^n), \phi^{n+1} - \phi^n \rangle.
\end{aligned}
\tag{2.9}
$$

For the term $\varepsilon^2\langle J*(\phi^{n+1}-\phi^n),\phi^{n+1}-\phi^n\rangle$, we apply Lemma 2.1 and obtain

$$
\begin{aligned}
\varepsilon^2\langle J*(\phi^{n+1}-\phi^n),\phi^{n+1}-\phi^n\rangle &= -\varepsilon^2\langle J*(\phi^{n+1}-\phi^n),\Delta_N((-\Delta_N)^{-1}(\phi^{n+1}-\phi^n))\rangle \\
&\leqslant \frac{1}{2}C_J\varepsilon^4\Delta t\|\phi^{n+1}-\phi^n\|_2^2 + \frac{2}{\Delta t}\|\nabla_N(-\Delta_N)^{-1}(\phi^{n+1}-\phi^n)\|_2^2 \\
&= \frac{1}{2}C_J\varepsilon^4\Delta t\|\phi^{n+1}-\phi^n\|_2^2 + \frac{2}{\Delta t}\|\phi^{n+1}-\phi^n\|_{-1,N}^2, \qquad (2.10)
\end{aligned}
$$

where C_J depends only on J and Ω. Subsequently, a combination of (2.9)–(2.10) yields

$$
\begin{aligned}
\varepsilon^2\langle \mathscr{L}_N\phi^{n+1},\phi^{n+1}-\phi^n\rangle &\geqslant \frac{\varepsilon^2}{2}(\langle \mathscr{L}_N\phi^{n+1},\phi^{n+1}\rangle - \langle \mathscr{L}_N\phi^n,\phi^n\rangle) \\
&\quad + \left(\frac{\varepsilon^2}{2}(J*1) - \frac{1}{4}C_J\varepsilon^4\Delta t\right)\|\phi^{n+1}-\phi^n\|_2^2 - \frac{1}{\Delta t}\|\phi^{n+1}-\phi^n\|_{-1,N}^2. \quad (2.11)
\end{aligned}
$$

For the nonlinear inner product, we begin with the following decomposition:

$$
(\breve{\phi}^{n+1})^3 - (\phi^{n+1})^3 = -((\breve{\phi}^{n+1})^2 + \breve{\phi}^{n+1}\phi^{n+1} + (\phi^{n+1})^2)(\phi^{n+1}-2\phi^n+\phi^{n-1}),
$$

where we have used the identity (2.7) again. In turn, the following estimate can be derived:

$$
\begin{aligned}
\langle (\breve{\phi}^{n+1})^3 &- (\phi^{n+1})^3,\phi^{n+1}-\phi^n\rangle \\
&\geqslant -\|(\breve{\phi}^{n+1})^2 + \breve{\phi}^{n+1}\phi^{n+1} + (\phi^{n+1})^2\|_\infty \cdot \|\phi^{n+1}-2\phi^n+\phi^{n-1}\|_2 \cdot \|\phi^{n+1}-\phi^n\|_2 \\
&\geqslant -\frac{3}{2}(\|\breve{\phi}^{n+1}\|_\infty^2 + \|\phi^{n+1}\|_\infty^2) \cdot \|\phi^{n+1}-2\phi^n+\phi^{n-1}\|_2 \cdot \|\phi^{n+1}-\phi^n\|_2 \\
&\geqslant -\frac{9}{4\gamma_0}(\|\breve{\phi}^{n+1}\|_\infty^2 + \|\phi^{n+1}\|_\infty^2)^2\|\phi^{n+1}-2\phi^n+\phi^{n-1}\|_2^2 - \frac{\gamma_0}{4}\|\phi^{n+1}-\phi^n\|_2^2. \qquad (2.12)
\end{aligned}
$$

Meanwhile, the following estimate is straightforward:

$$
\langle (\phi^{n+1})^3,\phi^{n+1}-\phi^n\rangle \geqslant \frac{1}{4}(\|\phi^{n+1}\|_4^4 - \|\phi^n\|_4^4), \qquad (2.13)
$$

which comes directly from the convexity of $\|\phi\|_4^4$ (in term of ϕ). Therefore, a combination of (2.12)–(2.13) yields

$$
\begin{aligned}
\langle (\breve{\phi}^{n+1})^3,\phi^{n+1}-\phi^n\rangle &\geqslant \frac{1}{4}(\|\phi^{n+1}\|_4^4 - \|\phi^n\|_4^4) - \frac{\gamma_0}{4}\|\phi^{n+1}-\phi^n\|_2^2 \\
&\quad - \frac{9}{4\gamma_0}(\|\breve{\phi}^{n+1}\|_\infty^2 + \|\phi^{n+1}\|_\infty^2)^2\|\phi^{n+1}-2\phi^n+\phi^{n-1}\|_2^2. \qquad (2.14)
\end{aligned}
$$

Finally, a substitution of (2.5), (2.6), (2.8), (2.11) and (2.14) into (2.4) gives

$$\frac{1}{4\Delta t}(\|\phi^{n+1} - \phi^n\|_{-1,N}^2 - \|\phi^n - \phi^{n-1}\|_{-1,N}^2) + \frac{A+1}{2}(\|\phi^{n+1} - \phi^n\|_2^2 - \|\phi^n - \phi^{n-1}\|_2^2)$$

$$+ E_N(\phi^{n+1}) - E_N(\phi^n) + \left(\frac{1}{2}(\varepsilon^2(J*1) - 1) - \frac{\gamma_0}{4} - \frac{1}{4}C_J\varepsilon^4\Delta t\right)\|\phi^{n+1} - \phi^n\|_2^2$$

$$+ \left(\frac{A+1}{2} - \frac{9}{4\gamma_0}(\|\breve{\phi}^{n+1}\|_\infty^2 + \|\phi^{n+1}\|_\infty^2)^2\right)\|\phi^{n+1} - 2\phi^n + \phi^{n-1}\|_2^2 \leqslant 0.$$

Making use of the assumption $\gamma_0 = \varepsilon^2(J*1) - 1 > 0$ (given by (1.4)), we get

$$\tilde{E}_N(\phi^{n+1}, \phi^n) - \tilde{E}_N(\phi^n, \phi^{n-1}) + \left(\frac{\gamma_0}{4} - \frac{1}{4}C_J\varepsilon^4\Delta t\right)\|\phi^{n+1} - \phi^n\|_2^2$$

$$+ \left(\frac{A+1}{2} - \frac{9}{4\gamma_0}(\|\breve{\phi}^{n+1}\|_\infty^2 + \|\phi^{n+1}\|_\infty^2)^2\right)\|\phi^{n+1} - 2\phi^n + \phi^{n-1}\|_2^2 \leqslant 0.$$

Consequently, under the constraint (2.3), a modified energy stability estimate (2.2) is valid. This completes the proof of Proposition 2.2. □

Note that the right-hand side of (2.3) involves the ℓ^∞ norms of the numerical solutions ϕ^{n-1}, ϕ^n and ϕ^{n+1}. Therefore, we have to justify the lower bound of A by estimating these ℓ^∞ norms. As mentioned before, a direct analysis given in Li *et al.* (2016) and Li & Qiao (2017a,b) for the classic Cahn–Hilliard equation may be difficult to be extended to (2.1) due to the lack of higher order diffusion terms. Instead, by resorting to the idea that the numerical solution can be regarded as a perturbation of the exact solution, we will perform a local-in-time convergence analysis of (2.1) and then give the ℓ^∞ bound of the numerical solution by using the convergence result.

3. Convergence analysis

We use Φ to denote the exact solution to the NCH equation (1.3). The existence and uniqueness of Φ may be established in a similar technique adopted in Bates & Han (2005a,b), and one can obtain

$$\|\Phi\|_{L^\infty(0,T;L^\infty)} + \|\Phi_t\|_{L^\infty(0,T;L^\infty)} \leqslant C, \tag{3.1}$$

for any $T > 0$. Without loss of generality, we consider the two-dimensional case.

First, we introduce the (spatial) Fourier projection of the exact solution, which satisfies the discrete mass-conserving property. Let $\mathscr{B}^K$ be the space of trigonometric polynomials of degree up to $K = N/2$. For a fixed time t, let $\Phi_N(\cdot, t) := \mathscr{P}_N\Phi(\cdot, t)$ be the Fourier projection of the exact solution into $\mathscr{B}^K$. Since $1 \in \mathscr{B}^K$, we have a useful property for the Fourier projection:

$$\int_\Omega \Phi_N(\cdot, t)\, d\mathbf{x} = \int_\Omega \Phi(\cdot, t)\, d\mathbf{x}. \tag{3.2}$$

If $\Phi \in L^{\infty}(0, T; H^{\ell}_{\text{per}})$ for some $\ell \in \mathbb{N}$, the projection approximation is standard:

$$\|\Phi_N - \Phi\|_{L^{\infty}(0,T;H^k)} \leqslant Ch^{\ell-k}\|\Phi\|_{L^{\infty}(0,T;H^{\ell})}, \quad 0 \leqslant k \leqslant \ell. \tag{3.3}$$

Then, the rest of the work is to estimate the difference between the numerical solution and the projection solution Φ_N.

Denote $\Phi_N^k = \Phi_N(\cdot, t_k)$. We denote by $\phi_N^k := \mathscr{P}_h \Phi_N(\cdot, t_k)$ the values of Φ_N at discrete grid points at time t_k. By (3.2) and the fact that the exact solution Φ is mass conservative at the continuous level, we have

$$\int_{\Omega} \Phi_N(\cdot, t_k) \, \mathrm{d}\mathbf{x} = \int_{\Omega} \Phi(\cdot, t_k) \, \mathrm{d}\mathbf{x} = \int_{\Omega} \Phi(\cdot, t_{k-1}) \, \mathrm{d}\mathbf{x} = \int_{\Omega} \Phi_N(\cdot, t_{k-1}) \, \mathrm{d}\mathbf{x}, \quad \forall \, k \in \mathbb{N}.$$

Meanwhile, since $\Phi_N \in \mathscr{B}^K$ and (3.2), the mass conservative property is available at the discrete level:

$$\overline{\phi_N^k} = \frac{1}{|\Omega|} \int_{\Omega} \Phi_N(\cdot, t_k) \, \mathrm{d}\mathbf{x} = \frac{1}{|\Omega|} \int_{\Omega} \Phi_N(\cdot, t_{k-1}) \, \mathrm{d}\mathbf{x} = \overline{\phi_N^{k-1}}, \quad \forall \, k \in \mathbb{N}.$$

For the initial value ϕ^0 of the numerical scheme (2.1), we apply the mass conservative projection: $\phi^0 = \mathscr{P}_h \Phi_N(\cdot, t = 0)$, that is, $\phi_{i,j}^0 := \Phi_N(x_i, y_j, t = 0)$. Then, the solution of the numerical scheme (2.1) is mass conservative, i.e.,

$$\overline{\phi^k} = \overline{\phi^{k-1}}, \quad \forall \, k \in \mathbb{N}.$$

And also, corresponding to the regularity (3.1), we have

$$\max_{1 \leqslant j \leqslant N_k} \left\|\phi_N^j\right\|_{\infty} + \max_{1 \leqslant j \leqslant N_k} \left\|\frac{\phi_N^j - \phi_N^{j-1}}{\Delta t}\right\|_{\infty} < C^*.$$

Notice that the constant C^* depends on $\|\Phi\|_{C^1(0,T;H^2)}$, with an application of two-dimensional Sobolev inequality. Since ϕ_N^k and Φ_N^k have the same values on the discrete grid points, we just use the notation Φ_N^k in the following discussions, for the sake of brevity.

With initial data of sufficient regularity, we can assume that the exact solution has regularity as

$$\Phi \in \mathscr{R} := H^5(0, T; C^0_{\text{per}}) \cap H^4(0, T; C^2_{\text{per}}) \cap L^{\infty}(0, T; C^{m+2}_{\text{per}}), \quad m \geqslant 3.$$

The following theorem is the main result on the error estimates of the stabilized BDF2 scheme (2.1).

THEOREM 3.1   Suppose the unique, smooth, periodic solution for the NCH equation (1.3), given by $\Phi(x, y, t)$ on Ω for $0 < t < \infty$, is of regularity class $\mathscr{R}$. In addition, the constant A is assumed to satisfy

$$A \geqslant \frac{18(M_0 + 1)^4}{\gamma_0} - 1, \quad \text{with } M_0 = 1 + C^*, \; C^* = \max_{1 \leqslant j \leqslant N_k} (\|\Phi_N^j\|_{\infty} + \|\partial_t \Phi_N^j\|_{\infty}). \tag{3.4}$$

Then, if Δt and h are sufficiently small, under linear refinement path constraint $C_1 h \leqslant \Delta t \leqslant C_2 h$ with fixed constants C_1 and C_2, we have

$$\|\Phi_N^n - \phi^n\|_2 \leqslant C(\Delta t^2 + h^m), \tag{3.5}$$

for all positive integers n such that $n\Delta t \leqslant T$, where C is independent of h and Δt.

The detailed proof will be presented in the following subsections. First, we will conduct the higher order consistency analysis to provide a high order truncation error so that the desired order of error can be recovered by using the inverse inequality. In fact, this approach has been adopted for the numerical analysis of a large family of nonlinear PDEs, see, e.g., E & Liu (1995), Samelson *et al.* (2003), Wang *et al.* (2004), Baskaran *et al.* (2013), Guan *et al.* (2014b), Wang *et al.* (2015), Guan *et al.* (2017), Duan *et al.* (2020), Duan *et al.* (2021) and Liu *et al.* (2021). Subsequently, we carry out the stability estimates for the numerical error function. Due to the complexity of the nonlinear term, it seems difficult to obtain the expected results directly, so we have to divide this part into two steps: a rough estimate is first performed in order to give the ℓ^∞ norms of the numerical solution, then a refined estimate is given, combined with the ℓ^∞ bound obtained by the rough estimate, to derive the desired result of convergence rate. In addition, instead of testing the error equation by $(-\Delta_N)^{-1}\hat{e}^{n+1}$ as usual, we adopt a novel test function $(-\Delta_N)^{-1}(\hat{e}^{n+1} - \hat{e}^n)$ so that a higher-order temporal truncation error can be obtained to match the second-order BDF discretization of the temporal derivative. This part is significantly different from the stability estimate in a recent work (Li *et al.*, 2021).

3.1 *Higher-order consistency analysis*

By consistency, the Fourier projection solution Φ_N satisfies the discrete equation

$$\frac{\frac{3}{2}\Phi_N^{n+1} - 2\Phi_N^n + \frac{1}{2}\Phi_N^{n-1}}{\Delta t} = \Delta_N\left((\check{\Phi}_N^{n+1})^3 - \check{\Phi}_N^{n+1} + A(\Phi_N^{n+1} - 2\Phi_N^n + \Phi_N^{n-1}) + \varepsilon^2 \mathscr{L}_N\Phi_N^{n+1}\right) + \tau_0^{n+1},$$

where $\check{\Phi}_N^{n+1} = 2\Phi_N^n - \Phi_N^{n-1}$ and τ_0^{n+1} is the truncation error satisfying $\|\tau_0^{n+1}\|_{-1,N} \leqslant C(\Delta t^2 + h^m)$. With the standard stability estimates, one can bound the H_h^{-1} norm of the numerical error $\Phi_N^n - \phi^n$ by the same order $O(\Delta t^2 + h^m)$. However, this convergence order is not enough to recover the ℓ^∞ bound of the numerical solution and its discrete temporal derivative after the inverse inequality is used. To overcome this difficulty, we will construct a supplementary field to correct Φ_N so that a higher $O(\Delta t^3 + h^m)$ consistency can be obtained, which is enough to recover the ℓ^∞ bound of the numerical solution.

According to the consistency, applying the temporal discretization in (2.1) to the Fourier projection solution Φ_N, we can get

$$\frac{\frac{3}{2}\Phi_N^{n+1} - 2\Phi_N^n + \frac{1}{2}\Phi_N^{n-1}}{\Delta t} = \Delta\left((\check{\Phi}_N^{n+1})^3 - \check{\Phi}_N^{n+1} + A(\Phi_N^{n+1} - 2\Phi_N^n + \Phi_N^{n-1}) + \varepsilon^2 \mathscr{L}\Phi_N^{n+1}\right)$$
$$+ \Delta t^2 (\mathbf{g}^{(2)})^{n+1} + O(\Delta t^3) + O(h^m), \tag{3.6}$$

where the function $\mathbf{g}^{(2)}(x, y, t)$ is sufficiently smooth and depends only on the higher-order partial derivatives of Φ_N by using the Taylor expansion in time.

With given profile $(\Phi_N)^2$, we define the temporal correction function $\Phi_{\Delta t}^{(2)}$ as the solution of the equation

$$\partial_t \Phi_{\Delta t}^{(2)} = \Delta\Big(3(\Phi_N)^2\Phi_{\Delta t}^{(2)} - \Phi_{\Delta t}^{(2)} + \varepsilon^2\mathscr{L}\Phi_{\Delta t}^{(2)}\Big) - g^{(2)}, \tag{3.7}$$

subject to the zero initial value and the periodic boundary condition. Note that (3.7) is a linear parabolic equation, so that the existence and uniqueness of $\Phi_{\Delta t}^{(2)}$ can be guaranteed by conducting the Galerkin approximation and Sobolev estimates (Temam, 2001). In addition, the solution $\Phi_{\Delta t}^{(2)}$ is smooth enough and depends only on Φ_N. Then, applying the temporal discretization to (3.7), we get

$$\frac{\frac{3}{2}(\Phi_{\Delta t}^{(2)})^{n+1} - 2(\Phi_{\Delta t}^{(2)})^n + \frac{1}{2}(\Phi_{\Delta}^{(2)}t)^{n-1}}{\Delta t}$$
$$= \Delta\Big(3(\check{\Phi}_N^{n+1})^2(\check{\Phi}_{\Delta t}^{(2)})^{n+1} - (\check{\Phi}_{\Delta t}^{(2)})^{n+1} + A((\Phi_{\Delta t}^{(2)})^{n+1} - 2(\Phi_{\Delta t}^{(2)})^n + (\Phi_{\Delta t}^{(2)})^{n-1})$$
$$+ \varepsilon^2\mathscr{L}(\Phi_{\Delta t}^{(2)})^{n+1}\Big) - (g^{(2)})^{n+1} + O(\Delta t^2), \tag{3.8}$$

where $(\check{\Phi}_{\Delta t}^{(2)})^{n+1} = 2(\Phi_{\Delta t}^{(2)})^n - (\Phi_{\Delta t}^{(2)})^{n-1}$. Subsequently, a correction of Φ is defined as

$$\hat{\Phi} = \Phi_N + \Delta t^2 \mathscr{P}_N\Phi_{\Delta t}^{(2)}. \tag{3.9}$$

It is clear that $\hat{\Phi}(\,\cdot\,,t) \in \mathscr{B}^K$ and $\hat{\Phi}$ satisfies the mass conservation property. Multiplying the Fourier projection of (3.8) by Δt^2 and its sum with (3.6) leads to

$$\frac{\frac{3}{2}\hat{\Phi}^{n+1} - 2\hat{\Phi}^n + \frac{1}{2}\hat{\Phi}^{n-1}}{\Delta t} = \Delta\Big((\check{\hat{\Phi}}^{n+1})^3 - \check{\hat{\Phi}}^{n+1} + A(\hat{\Phi}^{n+1} - 2\hat{\Phi}^n + \hat{\Phi}^{n-1}) + \varepsilon^2\mathscr{L}\hat{\Phi}^{n+1}\Big)$$
$$+ O(\Delta t^3) + O(h^m),$$

where $\check{\hat{\Phi}}^{n+1} = 2\hat{\Phi}^n - \hat{\Phi}^{n-1}$ and we have used the fact that

$$(\check{\hat{\Phi}}^{n+1})^3 = \big(\check{\Phi}_N^{n+1} + \Delta t^2\mathscr{P}_N(\check{\Phi}_{\Delta t}^{(2)})^{n+1}\big)^3$$
$$= (\check{\Phi}_N^{n+1})^3 + 3\Delta t^2(\check{\Phi}_N^{n+1})^2\mathscr{P}_N(\check{\Phi}_{\Delta t}^{(2)})^{n+1} + O(\Delta t^4) + O(h^m)$$
$$= (\check{\Phi}_N^{n+1})^3 + 3\Delta t^2\mathscr{P}_N\big((\check{\Phi}_N^{n+1})^2\mathscr{P}_N(\check{\Phi}_{\Delta t}^{(2)})^{n+1}\big) + O(\Delta t^4) + O(h^m).$$

Finally, applying the spatial Fourier pseudo-spectral approximation, we obtain

$$\frac{\frac{3}{2}\hat{\Phi}^{n+1} - 2\hat{\Phi}^n + \frac{1}{2}\hat{\Phi}^{n-1}}{\Delta t} = \Delta_N\Big((\check{\hat{\Phi}}^{n+1})^3 - \check{\hat{\Phi}}^{n+1} + A(\hat{\Phi}^{n+1} - 2\hat{\Phi}^n + \hat{\Phi}^{n-1}) + \varepsilon^2\mathscr{L}_N\hat{\Phi}^{n+1}\Big) + \tau_2^{n+1}, \tag{3.10}$$

where τ_2^{n+1} is the truncation error satisfying $\|\tau_2^{n+1}\|_{-1,N} \leqslant C(\Delta t^3 + h^m)$. Note that $\|\tau_2^{n+1}\|_{-1,N}$ is well defined since $\tau_2^{n+1} \in \mathcal{M}_h^0$, which is because $\hat{\Phi}$ is mass-conserving.

For the correction $\hat{\Phi}$ defined by (3.9), a detailed analysis implies that

$$\|\hat{\Phi} - \Phi_N\|_\infty \leqslant \check{C}_0(\Delta t^2 + h^m),$$

since $\|\mathscr{P}_N \Phi_{\Delta t}^{(2)}\|_\infty \leqslant C$. Moreover, when Δt and h are sufficiently small so that

$$\check{C}_0(\Delta t^2 + h^m) \leqslant \frac{1}{2}, \quad \frac{2\check{C}_0(\Delta t^2 + h^m)}{\Delta t} \leqslant \frac{1}{2}, \quad \text{i.e. } \Delta t \leqslant \frac{1}{8\check{C}_0}, \ h \leqslant \left(\frac{C_1}{4\check{C}_0}\right)^{\frac{1}{m-1}}, \ C_1 h \leqslant \Delta t \leqslant C_2 h,$$

we have the following estimates:

$$\|\hat{\Phi} - \Phi_N\|_\infty \leqslant C(\Delta t^2 + h^m) \leqslant \frac{1}{2} \implies \|\hat{\Phi}\|_\infty \leqslant \|\Phi_N\|_\infty + \|\hat{\Phi} - \Phi_N\|_\infty \leqslant C^* + \frac{1}{2}, \qquad (3.11)$$

$$\left\|\frac{\hat{\Phi}^j - \hat{\Phi}^{j-1}}{\Delta t} - \frac{\Phi_N^j - \Phi_N^{j-1}}{\Delta t}\right\|_\infty \leqslant \frac{1}{2} \implies \left\|\frac{\hat{\Phi}^j - \hat{\Phi}^{j-1}}{\Delta t}\right\|_\infty \leqslant C^* + \frac{1}{2}. \qquad (3.12)$$

In particular, an $O(\Delta t^3 + h^m)$ bound between the numerical solution ϕ and the projection solution Φ_N could be obtained at the first time step t_1:

$$\phi^1 - \Phi^1 = O(\Delta t^3 + h^m), \quad \Phi^1 - \Phi_N^1 = O(h^m), \quad \text{so that } \phi^1 - \Phi_N^1 = O(\Delta t^3 + h^m),$$

in which the first estimate, $\phi^1 - \Phi^1 = O(\Delta t^3 + h^m)$, comes from the fact that the RK2 numerical algorithm creates a third-order accurate numerical solution in the first step. Meanwhile, since a trivial zero initial data is imposed for $\Phi_{\Delta t}^{(2)}$, we observe that

$$(\Phi_{\Delta t}^{(2)})^1 = O(\Delta t + h^m).$$

In turn, the construction formula (3.9) implies that

$$\hat{\Phi}^1 = \Phi_N^1 + \Delta t^2 \mathscr{P}_N(\Phi_{\Delta t}^{(2)})^1 = \Phi_N^1 + O(\Delta t^3 + h^m).$$

Then we arrive at the following estimate at the first time step t_1:

$$\phi^1 - \hat{\Phi}^1 = O(\Delta t^3 + h^m), \quad \text{i.e. } \|\phi^1 - \hat{\Phi}^1\|_2 \leqslant C(\Delta t^3 + h^m). \qquad (3.13)$$

3.2 A rough error estimate

We analyze the error between the numerical solution and the constructed solution $\hat{\Phi}$ to obtain a higher-order convergence in the ℓ^2 norm. Define the error function $\hat{e}^k := \hat{\Phi}^k - \phi^k$, then $\hat{e}^k \in \mathcal{M}_h^0$, and thus

$\|\hat{e}^k\|_{-1,N}$ is well defined for any k. The difference between (2.1) and (3.10) gives

$$\frac{\frac{3}{2}\hat{e}^{n+1} - 2\hat{e}^n + \frac{1}{2}\hat{e}^{n-1}}{\Delta t} = \Delta_N\Big((\check{\hat{\Phi}}^{n+1})^3 - (\check{\phi}^{n+1})^3 - \check{\hat{e}}^{n+1} + A(\hat{e}^{n+1} - 2\hat{e}^n + \hat{e}^{n-1}) + \varepsilon^2 \mathscr{L}_N \hat{e}^{n+1}\Big) + \tau_2^{n+1},$$
(3.14)

where $\check{\hat{e}}^{n+1} = 2\hat{e}^n - \hat{e}^{n-1}$. To estimate the nonlinear terms, we make an assumption for the numerical error function in the ℓ^2 and H_h^{-1} norms at the previous time steps t_n, t_{n-1}:

$$\|\hat{e}^k\|_2 \leqslant \Delta t^{\frac{19}{8}} + h^{m-\frac{3}{4}} \ (k = n, n-1), \quad \frac{1}{\Delta t^{\frac{1}{2}}}\|\hat{e}^n - \hat{e}^{n-1}\|_{-1,N} \leqslant \Delta t^{\frac{19}{8}} + h^{m-\frac{3}{4}}. \tag{3.15}$$

Under the linear constraint $\Delta t \leqslant C_2 h$ enforced in Theorem 3.1, an application of two-dimensional inverse inequality reveals that

$$\|\hat{e}^k\|_\infty \leqslant \frac{C\|\hat{e}^k\|_2}{h} \leqslant C(\Delta t^{\frac{11}{8}} + h^{m-\frac{7}{4}}), \quad k = n, n-1. \tag{3.16}$$

Consequently, the ℓ^∞ bound for the numerical solutions at t_n and t_{n-1}, as well as their discrete temporal derivative, becomes available:

$$\|\phi^k\|_\infty \leqslant \|\hat{\Phi}^k\|_\infty + \|\hat{e}^k\|_\infty \leqslant C^* + \frac{1}{2} + \frac{1}{2} = M_0 \ (k = n, n-1), \tag{3.17}$$

$$\left\|\frac{\phi^n - \phi^{n-1}}{\Delta t}\right\|_\infty \leqslant \left\|\frac{\hat{\Phi}^n - \hat{\Phi}^{n-1}}{\Delta t}\right\|_\infty + \left\|\frac{\hat{e}^n - \hat{e}^{n-1}}{\Delta t}\right\|_\infty \leqslant C^* + \frac{1}{2} + C(\Delta t^{\frac{3}{8}} + h^{m-\frac{11}{4}})$$

$$\leqslant C^* + \frac{1}{2} + \frac{1}{2} = M_0, \tag{3.18}$$

where (3.11) and (3.12) have been used. The *a priori* assumption (3.15) will be recovered in the convergence analysis presented later.

It is noticed that the *a priori* $\|\cdot\|_\infty$ assumption (3.15) is valid at $k = 0, 1$ and $n = 1$, which comes from the fact that $\hat{e}^0 \equiv 0$, and the initial error estimate (3.13) (at the first time step t_1), combined with the linear refinement requirement, $C_1 h \leqslant \Delta t \leqslant C_2 h$.

Taking a discrete inner product with (3.14) by $(-\Delta_N)^{-1}(\hat{e}^{n+1} - \hat{e}^n)$ leads to

$$\frac{1}{\Delta t}\Big\langle \frac{3}{2}\hat{e}^{n+1} - 2\hat{e}^n + \frac{1}{2}\hat{e}^{n-1}, \hat{e}^{n+1} - \hat{e}^n \Big\rangle_{-1,N} + A\langle \hat{e}^{n+1} - 2\hat{e}^n + \hat{e}^{n-1}, \hat{e}^{n+1} - \hat{e}^n \rangle$$

$$= -\langle (\check{\hat{\Phi}}^{n+1})^3 - (\check{\phi}^{n+1})^3, \hat{e}^{n+1} - \hat{e}^n \rangle + \langle \check{\hat{e}}^{n+1}, \hat{e}^{n+1} - \hat{e}^n \rangle - \varepsilon^2 \langle \mathscr{L}_N \hat{e}^{n+1}, \hat{e}^{n+1} - \hat{e}^n \rangle$$

$$+ \langle \tau_2^{n+1}, \hat{e}^{n+1} - \hat{e}^n \rangle_{-1,N}. \tag{3.19}$$

For the left-hand side term associated with the temporal stencil, the following estimate is straightforward:

$$\left\langle \frac{3}{2}\hat{e}^{n+1} - 2\hat{e}^n + \frac{1}{2}\hat{e}^{n-1}, \hat{e}^{n+1} - \hat{e}^n \right\rangle_{-1,N} = \left\langle \frac{3}{2}(\hat{e}^{n+1} - \hat{e}^n) - \frac{1}{2}(\hat{e}^n - \hat{e}^{n-1}), \hat{e}^{n+1} - \hat{e}^n \right\rangle_{-1,N}$$

$$\geqslant \frac{3}{2}\|\hat{e}^{n+1} - \hat{e}^n\|_{-1,N}^2 - \frac{1}{4}(\|\hat{e}^{n+1} - \hat{e}^n\|_{-1,N}^2 + \|\hat{e}^n - \hat{e}^{n-1}\|_{-1,N}^2)$$

$$\geqslant \frac{5}{4}\|\hat{e}^{n+1} - \hat{e}^n\|_{-1,N}^2 - \frac{1}{4}\|\hat{e}^n - \hat{e}^{n-1}\|_{-1,N}^2. \tag{3.20}$$

For the artificial regularization term, we have the following identity:

$$\langle \hat{e}^{n+1} - 2\hat{e}^n + \hat{e}^{n-1}, \hat{e}^{n+1} - \hat{e}^n \rangle = \frac{1}{2}(\|\hat{e}^{n+1} - \hat{e}^n\|_2^2 - \|\hat{e}^n - \hat{e}^{n-1}\|_2^2 + \|\hat{e}^{n+1} - 2\hat{e}^n + \hat{e}^{n-1}\|_2^2).$$

The last term on the right-hand side of (3.19) can be bounded by

$$\langle \tau_2^{n+1}, \hat{e}^{n+1} - \hat{e}^n \rangle_{-1,N} \leqslant \|\hat{e}^{n+1} - \hat{e}^n\|_{-1,N} \cdot \|\tau_2^{n+1}\|_{-1,N} \leqslant \frac{1}{4\Delta t}\|\hat{e}^{n+1} - \hat{e}^n\|_{-1,N}^2 + \Delta t\|\tau_2^{n+1}\|_{-1,N}^2.$$

For the second linear term on the right-hand side, a direct computation gives

$$\langle \check{\hat{e}}^{n+1}, \hat{e}^{n+1} - \hat{e}^n \rangle = \langle \hat{e}^{n+1}, \hat{e}^{n+1} - \hat{e}^n \rangle - \langle \hat{e}^{n+1} - 2\hat{e}^n + \hat{e}^{n-1}, \hat{e}^{n+1} - \hat{e}^n \rangle$$

$$= \frac{1}{2}(\|\hat{e}^{n+1}\|_2^2 - \|\hat{e}^n\|_2^2 + \|\hat{e}^{n+1} - \hat{e}^n\|_2^2)$$

$$- \frac{1}{2}(\|\hat{e}^{n+1} - \hat{e}^n\|_2^2 - \|\hat{e}^n - \hat{e}^{n-1}\|_2^2 + \|\hat{e}^{n+1} - 2\hat{e}^n + \hat{e}^{n-1}\|_2^2), \tag{3.21}$$

where we have used the fact that

$$\check{\hat{e}}^{n+1} = \hat{e}^{n+1} - (\hat{e}^{n+1} - 2\hat{e}^n + \hat{e}^{n-1}). \tag{3.22}$$

The nonlocal linear term on the right-hand side can be rewritten as

$$-\varepsilon^2 \langle \mathscr{L}_N \hat{e}^{n+1}, \hat{e}^{n+1} - \hat{e}^n \rangle = -\varepsilon^2 \langle (J * 1)\hat{e}^{n+1} - J * \hat{e}^{n+1}, \hat{e}^{n+1} - \hat{e}^n \rangle$$

$$= -\varepsilon^2 (J * 1)\langle \hat{e}^{n+1}, \hat{e}^{n+1} - \hat{e}^n \rangle + \varepsilon^2 \langle J * \hat{e}^{n+1}, \hat{e}^{n+1} - \hat{e}^n \rangle. \tag{3.23}$$

For the first term appearing in above, the following identity is obvious:

$$\langle \hat{e}^{n+1}, \hat{e}^{n+1} - \hat{e}^n \rangle = \frac{1}{2}(\|\hat{e}^{n+1}\|_2^2 - \|\hat{e}^n\|_2^2 + \|\hat{e}^{n+1} - \hat{e}^n\|_2^2).$$

Meanwhile, for the term $\varepsilon^2 \langle J * \hat{e}^{n+1}, \hat{e}^{n+1} - \hat{e}^n \rangle$, we apply Lemma 2.1 and obtain

$$
\begin{aligned}
\varepsilon^2 \langle J * \hat{e}^{n+1}, \hat{e}^{n+1} - \hat{e}^n \rangle &= -\varepsilon^2 \langle J * \hat{e}^{n+1}, \Delta_N((-\Delta_N)^{-1}(\hat{e}^{n+1} - \hat{e}^n)) \rangle \\
&\leqslant C_3 \Delta t \|\hat{e}^{n+1}\|_2^2 + \frac{1}{4\Delta t} \|\nabla_N(-\Delta_N)^{-1}(\hat{e}^{n+1} - \hat{e}^n)\|_2^2 \\
&\leqslant C_3 \Delta t \|\hat{e}^{n+1}\|_2^2 + \frac{1}{4\Delta t} \|\hat{e}^{n+1} - \hat{e}^n\|_{-1,N}^2,
\end{aligned}
\tag{3.24}
$$

where C_3 depends only on C_J and ε. Subsequently, a combination of (3.23)-(3.24) yields

$$
\begin{aligned}
-\varepsilon^2 \langle \mathscr{L}_N \hat{e}^{n+1}, \hat{e}^{n+1} - \hat{e}^n \rangle &\leqslant -\frac{1}{2}\varepsilon^2 (J * 1)(\|\hat{e}^{n+1}\|_2^2 - \|\hat{e}^n\|_2^2 + \|\hat{e}^{n+1} - \hat{e}^n\|_2^2) \\
&\quad + C_3 \Delta t \|\hat{e}^{n+1}\|_2^2 + \frac{1}{4\Delta t} \|\hat{e}^{n+1} - \hat{e}^n\|_{-1,N}^2.
\end{aligned}
\tag{3.25}
$$

For the nonlinear inner product on the right-hand side of (3.19), we begin with the following nonlinear expansion:

$$
(\check{\hat{\phi}}^{n+1})^3 - (\check{\phi}^{n+1})^3 = ((\check{\hat{\phi}}^{n+1})^2 + \check{\hat{\phi}}^{n+1}\check{\phi}^{n+1} + (\check{\phi}^{n+1})^2)\check{\hat{e}}^{n+1}.
\tag{3.26}
$$

The consistency estimates (3.11) and (3.12), and *a priori* estimates (3.17) and (3.18) indicate that

$$
\|\check{\hat{\phi}}^{n+1}\|_\infty \leqslant C^* + \frac{1}{2} + \frac{1}{2} = M_0, \quad \|\check{\phi}^{n+1}\|_\infty \leqslant C^* + 1 + \frac{1}{2} \leqslant M_0 + 1,
$$

which in turn leads to

$$
\|(\check{\hat{\phi}}^{n+1})^2 + \check{\hat{\phi}}^{n+1}\check{\phi}^{n+1} + (\check{\phi}^{n+1})^2\|_\infty \leqslant 3(M_0 + 1)^2.
\tag{3.27}
$$

Then, we arrive at

$$
\|(\check{\hat{\phi}}^{n+1})^3 - (\check{\phi}^{n+1})^3\|_2 \leqslant \|(\check{\hat{\phi}}^{n+1})^2 + \check{\hat{\phi}}^{n+1}\check{\phi}^{n+1} + (\check{\phi}^{n+1})^2\|_\infty \cdot \|\check{\hat{e}}^{n+1}\|_2 \leqslant 3(M_0 + 1)^2\|\check{\hat{e}}^{n+1}\|_2.
$$

As a consequence, the following rough estimate is available:

$$
\begin{aligned}
-\langle (\check{\hat{\phi}}^{n+1})^3 - (\check{\phi}^{n+1})^3, \hat{e}^{n+1} - \hat{e}^n \rangle &\leqslant \|(\check{\hat{\phi}}^{n+1})^3 - (\check{\phi}^{n+1})^3\|_2 \cdot \|\hat{e}^{n+1} - \hat{e}^n\|_2 \\
&\leqslant 3(M_0 + 1)^2\|\check{\hat{e}}^{n+1}\|_2 \cdot \|\hat{e}^{n+1} - \hat{e}^n\|_2 \\
&\leqslant 9(M_0 + 1)^4 \gamma_0^{-1}\|\check{\hat{e}}^{n+1}\|_2^2 + \frac{\gamma_0}{4}\|\hat{e}^{n+1} - \hat{e}^n\|_2^2.
\end{aligned}
\tag{3.28}
$$

Therefore, by substituting (3.20)-(3.21), (3.25) and (3.28) into (3.19), we obtain

$$\frac{3}{4\Delta t}\|\hat{e}^{n+1} - \hat{e}^n\|^2_{-1,N} - \frac{1}{4\Delta t}\|\hat{e}^n - \hat{e}^{n-1}\|^2_{-1,N} + \frac{A+1}{2}(\|\hat{e}^{n+1} - \hat{e}^n\|^2_2 - \|\hat{e}^n - \hat{e}^{n-1}\|^2_2)$$

$$+ \frac{1}{2}(\varepsilon^2(J*1) - 1)(\|\hat{e}^{n+1}\|^2_2 - \|\hat{e}^n\|^2_2 + \|\hat{e}^{n+1} - \hat{e}^n\|^2_2) - \frac{\gamma_0}{4}\|\hat{e}^{n+1} - \hat{e}^n\|^2_2$$

$$\leqslant C_3\Delta t\|\hat{e}^{n+1}\|^2_2 + 9(M_0 + 1)^4\gamma_0^{-1}\|\check{e}^{n+1}\|_2 + \Delta t\|\tau_2^{n+1}\|^2_{-1,N}. \tag{3.29}$$

Making use of the assumption $\gamma_0 = \varepsilon^2(J*1) - 1 > 0$ (given by (1.4)), we get

$$\frac{\gamma_0}{2}\|\hat{e}^{n+1}\|^2_2 \leqslant \frac{1}{4\Delta t}\|\hat{e}^n - \hat{e}^{n-1}\|^2_{-1,N} + \frac{A+1}{2}\|\hat{e}^n - \hat{e}^{n-1}\|^2_2 + \frac{\gamma_0}{2}\|\hat{e}^n\|^2_2$$

$$+ C_3\Delta t\|\hat{e}^{n+1}\|^2_2 + 9(M_0 + 1)^4\gamma_0^{-1}\|\check{e}^{n+1}\|^2_2 + \Delta t\|\tau_2^{n+1}\|^2_{-1,N}.$$

Meanwhile, with the application of the *a priori* error estimate (3.15), we arrive at

$$\frac{\gamma_0}{4}\|\hat{e}^{n+1}\|^2_2 \leqslant C_4(\Delta t^{\frac{9}{2}} + h^{2m-\frac{3}{2}}),$$

by combining with $\frac{A+1}{2} \leqslant \Delta t^{-\frac{1}{2}}$ and $C_3\Delta t \leqslant \frac{\gamma_0}{4}$ provided that Δt and h are sufficiently small, with a linear refinement constraint $C_1 h \leqslant \Delta t \leqslant C_2 h$. Subsequently, an application of two-dimensional inverse inequality implies that

$$\|\hat{e}^{n+1}\|_\infty \leqslant \frac{C\|\hat{e}^{n+1}\|_2}{h} \leqslant \hat{C}_1(\Delta t^{\frac{5}{4}} + h^{m-\frac{7}{4}}) \leqslant \Delta t, \quad \text{with } \hat{C}_1 := C(4C_4\gamma_0^{-1})^{1/2},$$

$$\text{provided that} \quad \Delta t \leqslant \left(\frac{1}{2\hat{C}_1}\right)^4, \quad h \leqslant \left(\frac{C_1}{2\hat{C}_1}\right)^{\frac{1}{m-\frac{11}{4}}} \quad \text{and } C_1 h \leqslant \Delta t \leqslant C_2 h, \tag{3.30}$$

under the same linear refinement requirement. As a consequence, the following *a priori* bounds can be derived:

$$\|\phi^{n+1}\|_\infty \leqslant \|\hat{\Phi}^{n+1}\|_\infty + \|\hat{e}^{n+1}\|_\infty \leqslant C^* + \frac{1}{2} + \frac{1}{2} = M_0, \tag{3.31}$$

$$\left\|\frac{\phi^{n+1} - \phi^n}{\Delta t}\right\|_\infty \leqslant \left\|\frac{\hat{\Phi}^{n+1} - \hat{\Phi}^n}{\Delta t}\right\|_\infty + \left\|\frac{\hat{e}^{n+1} - \hat{e}^n}{\Delta t}\right\|_\infty \leqslant C^* + \frac{1}{2} + \frac{1}{2} = M_0. \tag{3.32}$$

These bounds will play a crucial role in the refined error estimate.

3.3 *A refined error estimate*

In this subsection, we perform a more refined error estimate for the nonlinear term to improve the estimate (3.28), under the *a priori* estimate (3.32). As a result, an inductive argument can be applied to the inequality (3.29).

The following nonlinear expansion (3.26) is still available. We begin with the following rewritten form:

$$\langle(\check{\hat{\phi}}^{n+1})^3 - (\check{\phi}^{n+1})^3, \hat{e}^{n+1} - \hat{e}^n\rangle$$

$$= \langle((\check{\hat{\phi}}^{n+1})^2 + \check{\hat{\phi}}^{n+1}\check{\phi}^{n+1} + (\check{\phi}^{n+1})^2)\hat{e}^{n+1}, \hat{e}^{n+1} - \hat{e}^n\rangle$$

$$- \langle((\check{\hat{\phi}}^{n+1})^2 + \check{\hat{\phi}}^{n+1}\check{\phi}^{n+1} + (\check{\phi}^{n+1})^2)(\hat{e}^{n+1} - 2\hat{e}^n + \hat{e}^{n-1}), \hat{e}^{n+1} - \hat{e}^n\rangle, \qquad (3.33)$$

where we have used the identity (3.22). For the second term in (3.33), an application of (3.27) indicates that

$$- \langle((\check{\hat{\phi}}^{n+1})^2 + \check{\hat{\phi}}^{n+1}\check{\phi}^{n+1} + (\check{\phi}^{n+1})^2)(\hat{e}^{n+1} - 2\hat{e}^n + \hat{e}^{n-1}), \hat{e}^{n+1} - \hat{e}^n\rangle$$

$$\geqslant -3(M_0 + 1)^2\|\hat{e}^{n+1} - 2\hat{e}^n + \hat{e}^{n-1}\|_2 \cdot \|\hat{e}^{n+1} - \hat{e}^n\|_2$$

$$\geqslant -9(M_0 + 1)^4\gamma_0^{-1}\|\hat{e}^{n+1} - 2\hat{e}^n + \hat{e}^{n-1}\|_2^2 - \frac{\gamma_0}{4}\|\hat{e}^{n+1} - \hat{e}^n\|_2^2. \qquad (3.34)$$

For the first term in (3.33), we begin with the following obvious identity

$$\hat{e}^{n+1}(\hat{e}^{n+1} - \hat{e}^n) = \frac{1}{2}((\hat{e}^{n+1})^2 - (\hat{e}^n)^2 + (\hat{e}^{n+1} - \hat{e}^n)^2),$$

which in turn implies that

$$\langle((\check{\hat{\phi}}^{n+1})^2 + \check{\hat{\phi}}^{n+1}\check{\phi}^{n+1} + (\check{\phi}^{n+1})^2)\hat{e}^{n+1}, \hat{e}^{n+1} - \hat{e}^n\rangle$$

$$\geqslant \frac{1}{2}(\langle(\check{\hat{\phi}}^{n+1})^2 + \check{\hat{\phi}}^{n+1}\check{\phi}^{n+1} + (\check{\phi}^{n+1})^2, (\hat{e}^{n+1})^2\rangle - \langle(\check{\hat{\phi}}^{n+1})^2 + \check{\hat{\phi}}^{n+1}\check{\phi}^{n+1} + (\check{\phi}^{n+1})^2, (\hat{e}^n)^2\rangle)$$

$$= \frac{1}{2}\langle(\check{\hat{\phi}}^{n+1})^2 + \check{\hat{\phi}}^{n+1}\check{\phi}^{n+1} + (\check{\phi}^{n+1})^2, (\hat{e}^{n+1})^2\rangle - I_{nl}^n, \qquad (3.35)$$

where $I_{nl}^n := \frac{1}{2}\langle(\check{\hat{\phi}}^{n+1})^2 + \check{\hat{\phi}}^{n+1}\check{\phi}^{n+1} + (\check{\phi}^{n+1})^2, (\hat{e}^n)^2\rangle$. However, we observe that the first term in (3.35), $\frac{1}{2}\langle(\check{\hat{\phi}}^{n+1})^2 + \check{\hat{\phi}}^{n+1}\check{\phi}^{n+1} + (\check{\phi}^{n+1})^2, (\hat{e}^{n+1})^2\rangle$, is not equal to I_{nl}^{n+1}. To apply the induction analysis in later steps, we have to estimate their difference. The following inequalities come from the consistency estimate (3.12), and *a priori* estimates (3.18) and (3.32):

$$\|\hat{\Phi}^n - \hat{\Phi}^{n-1}\|_\infty, \ \|\hat{\Phi}^{n+1} - \hat{\Phi}^n\|_\infty, \ \|\phi^n - \phi^{n-1}\|_\infty, \ \|\phi^{n+1} - \phi^n\|_\infty \leqslant M_0\Delta t,$$

which in turn imply that

$$\|\check{\hat{\phi}}^{n+2} - \check{\hat{\phi}}^{n+1}\|_\infty \leqslant 3M_0\Delta t, \quad \|\check{\phi}^{n+2} - \check{\phi}^{n+1}\|_\infty \leqslant 3M_0\Delta t.$$

Moreover, the following estimates are available:

$$\|(\check{\hat{\phi}}^{n+2})^2 - (\check{\hat{\phi}}^{n+1})^2\|_\infty \leqslant \|\check{\hat{\phi}}^{n+2} + \check{\hat{\phi}}^{n+1}\|_\infty \cdot \|\check{\hat{\phi}}^{n+2} - \check{\hat{\phi}}^{n+1}\|_\infty \leqslant 2M_0 \cdot 3M_0\Delta t = 6M_0^2\Delta t.$$

With similar arguments, we get

$$\|\check{\hat{\phi}}^{n+2}\check{\phi}^{n+2} - \check{\hat{\phi}}^{n+1}\check{\phi}^{n+1}\|_\infty \leqslant 6M_0^2\Delta t, \quad \|(\check{\phi}^{n+2})^2 - (\check{\phi}^{n+1})^2\|_\infty \leqslant 6M_0^2\Delta t.$$

Then we arrive at

$$\|((\check{\hat{\phi}}^{n+2})^2 + \check{\hat{\phi}}^{n+2}\check{\phi}^{n+2} + (\check{\phi}^{n+2})^2) - ((\check{\hat{\phi}}^{n+1})^2 + \check{\hat{\phi}}^{n+1}\check{\phi}^{n+1} + (\check{\phi}^{n+1})^2)\|_\infty \leqslant 18M_0^2\Delta t.$$

As a direct consequence, the following bound is available:

$$\left| I_{nl}^{n+1} - \frac{1}{2}\langle (\check{\hat{\phi}}^{n+1})^2 + \check{\hat{\phi}}^{n+1}\check{\phi}^{n+1} + (\check{\phi}^{n+1})^2, (\hat{e}^{n+1})^2 \rangle \right| \leqslant 9M_0^2\Delta t\|\hat{e}^{n+1}\|_2^2.$$

Its substitution into (3.35) yields

$$\langle ((\check{\hat{\phi}}^{n+1})^2 + \check{\hat{\phi}}^{n+1}\check{\phi}^{n+1} + (\check{\phi}^{n+1})^2)\hat{e}^{n+1}, \hat{e}^{n+1} - \hat{e}^n \rangle \geqslant I_{nl}^{n+1} - I_{nl}^n - 9M_0^2\Delta t\|\hat{e}^{n+1}\|_2^2.$$

Combining with (3.33) and (3.34), we obtain a refined error estimate for the nonlinear inner product:

$$\langle (\check{\hat{\phi}}^{n+1})^3 - (\check{\phi}^{n+1})^3, \hat{e}^{n+1} - \hat{e}^n \rangle$$
$$\geqslant I_{nl}^{n+1} - I_{nl}^n - 9(M_0 + 1)^4\gamma_0^{-1}\|\hat{e}^{n+1} - 2\hat{e}^n + \hat{e}^{n-1}\|_2^2 - \frac{\gamma_0}{4}\|\hat{e}^{n+1} - \hat{e}^n\|_2^2 - 9M_0^2\Delta t\|\hat{e}^{n+1}\|_2^2. \quad (3.36)$$

As a result, a substitution of (3.20)-(3.21), (3.25) and (3.36) into (3.19) results in

$$\frac{3}{4\Delta t}\|\hat{e}^{n+1} - \hat{e}^n\|_{-1,N}^2 - \frac{1}{4\Delta t}\|\hat{e}^n - \hat{e}^{n-1}\|_{-1,N}^2$$
$$+ \frac{A+1}{2}(\|\hat{e}^{n+1} - \hat{e}^n\|_2^2 - \|\hat{e}^n - \hat{e}^{n-1}\|_2^2) + \frac{A+1}{2}\|\hat{e}^{n+1} - 2\hat{e}^n + \hat{e}^{n-1}\|_2^2 + I_{nl}^{n+1} - I_{nl}^n$$
$$+ \frac{1}{2}(\varepsilon^2(J * 1) - 1)(\|\hat{e}^{n+1}\|_2^2 - \|\hat{e}^n\|_2^2 + \|\hat{e}^{n+1} - \hat{e}^n\|_2^2) - \frac{\gamma_0}{2}\|\hat{e}^{n+1} - \hat{e}^n\|_2^2$$
$$\leqslant 9(M_0 + 1)^4\gamma_0^{-1}\|\hat{e}^{n+1} - 2\hat{e}^n + \hat{e}^{n-1}\|_2^2 + (C_3 + 9M_0^2)\Delta t\|\hat{e}^{n+1}\|_2^2 + \Delta t\|\tau_2^{n+1}\|_{-1,N}^2.$$

Considering $\gamma_0 = \varepsilon^2(J * 1) - 1 > 0$ and condition (3.4) for the parameter A, we get

$$
\frac{1}{4\Delta t}(\|\hat{e}^{n+1} - \hat{e}^n\|^2_{-1,N} - \|\hat{e}^n - \hat{e}^{n-1}\|^2_{-1,N})
$$

$$
+ \frac{A+1}{2}(\|\hat{e}^{n+1} - \hat{e}^n\|^2_2 - \|\hat{e}^n - \hat{e}^{n-1}\|^2_2) + I^{n+1}_{nl} - I^n_{nl} + \frac{\gamma_0}{2}(\|\hat{e}^{n+1}\|^2_2 - \|\hat{e}^n\|^2_2)
$$

$$
\leqslant (C_3 + 9M_0^2)\Delta t\|\hat{e}^{n+1}\|^2_2 + \Delta t\|\tau_2^{n+1}\|^2_{-1,N}.
$$

The following quantity is introduced:

$$
F^{n+1} := \frac{1}{4\Delta t}\|\hat{e}^{n+1} - \hat{e}^n\|^2_{-1,N} + \frac{A+1}{2}\|\hat{e}^{n+1} - \hat{e}^n\|^2_2 + I^{n+1}_{nl} + \frac{\gamma_0}{2}\|\hat{e}^{n+1}\|^2_2.
$$

Then we get the following estimate:

$$
F^{n+1} - F^n \leqslant C_5\Delta t F^{n+1} + \Delta t\|\tau_2^{n+1}\|^2_{-1,N}, \quad \text{with } C_5 = 2(C_3 + 9M_0^2)\gamma_0^{-1}.
$$

Using the discrete Gronwall inequality results in the desired convergence estimate:

$$
F^{n+1} \leqslant \hat{C}_2(\Delta t^6 + h^{2m}),
$$

since $\|\tau_2^j\|_{-1,N} \leqslant C(\Delta t^3 + h^m)$ for $j \leqslant n + 1$. In particular, we see that

$$
\|\hat{e}^{n+1}\|_2, \ \frac{1}{\Delta t^{\frac{1}{2}}}\|\hat{e}^{n+1} - \hat{e}^n\|_{-1,N} \leqslant C\hat{C}_2(\Delta t^3 + h^m) \leqslant \Delta t^{\frac{19}{8}} + h^{m-\frac{3}{4}}, \tag{3.37}
$$

so that the *a priori* assumption (3.15) has been recovered at time instant t_{n+1}. In turn, the analysis can be carried out in the induction style. This completes the error estimate for $\hat{e}$, the numerical error between the numerical solution ϕ and the constructed approximation solution $\hat{\Phi}$.

Finally, the error estimate (3.5) is a direct consequence of the following identity

$$
\Phi_N^k - \phi^k = \hat{e}^k - \Delta t^2(\mathscr{P}_N\Phi^{(2)}_{\Delta t})^k,
$$

which comes from the construction (3.9), as well as the fact that $\|(\mathscr{P}_N\Phi^{(2)}_{\Delta t})^k\|_2 \leqslant C$ for any $k \geqslant 0$. The proof of Theorem 3.1 is finished.

REMARK 3.2 The proof of Theorem 3.1 can be extended to the three-dimensional case without any essential difficulty. A key difference is an application of the three-dimensional inverse inequality, i.e.,

$$
\|\psi\|_\infty \leqslant \frac{C}{h^{\frac{3}{2}}}\|\psi\|_2, \quad \forall \psi \in \mathscr{M}_h,
$$

to revise the inequalities (3.16) and (3.30) accordingly. In addition, the quantities on the right-hand side of the inequalities in (3.15) have to be replaced by $\Delta t^{\frac{11}{4}} + h^{m-\frac{1}{4}}$. As a result, following the similar

derivations as the two-dimensional case, the last step of (3.37) can also be obtained by the same quantity, so that the induction process is completed.

3.4   *Theoretical justification of the energy stability*

As proved in Proposition 2.2, the numerical scheme (2.1) is energy stable under the condition (2.3), which involves the ℓ^∞ bound of the numerical solution. The proof of Theorem 3.1 implies that the ℓ^∞ bounds (3.17) and (3.31) for the numerical solution are available as long as another constraint (3.4) for A is valid. Thus, we can give a theoretical justification of the energy stability as follows.

COROLLARY 3.3   Under the assumptions of Theorem 3.1, the energy stability, namely $\tilde{E}_N(\phi^{n+1}, \phi^n) \leqslant \tilde{E}_N(\phi^n, \phi^{n-1})$, is valid under the constraint (3.4) for the regularization parameter A, combined with a trivial constraint for Δt: $C_J \varepsilon^4 \Delta t \leqslant \gamma_0$.

4. Numerical experiments

In this section, we conduct some numerical experiments by using the proposed stabilized BDF2 scheme (2.1) for solving the NCH equation (1.3) in the two-dimensional space. For the kernel involved in the nonlocal diffusion operator, as reported in Du *et al.* (2018), we use a family of Gauss-type functions, parameterized by a constant $\delta > 0$, taking the form

$$J_\delta(\mathbf{x}) = \frac{4}{\pi \delta^4} e^{-\frac{|\mathbf{x}|^2}{\delta^2}}, \quad \mathbf{x} \in \mathbb{R}^2. \tag{4.1}$$

Since $J_\delta * 1 = 4/\delta^2$, the condition (1.4) is equivalent to $\delta < 2\varepsilon$.

4.1   *Convergence tests*

First, we test the temporal convergence rate of the proposed scheme with different values of the parameters ε and δ.

EXAMPLE 4.1   Consider the NCH equation (1.3) in $\Omega = (-1, 1) \times (-1, 1)$ subject to periodic boundary condition and the initial value $\phi_0(x, y) = 0.5 \sin \pi x \sin \pi y + 0.1$ for the cases $\varepsilon^2 = 0.1$ and $\varepsilon^2 = 0.01$. The kernel (4.1) is adopted with $\delta^2 = \varepsilon^2$, $\delta^2 = 2\varepsilon^2$ and $\delta^2 = 3\varepsilon^2$, respectively. We test the temporal convergence rate of the scheme (2.1) by calculating the numerical solution at $t = 0.05$.

We adopt the uniform 1024×1024 spatial mesh. According to our observation in the numerical tests, such a spatial mesh is sufficiently fine so that the errors caused by the spatial approximation can be ignored. We compute the numerical solutions with various time step sizes $\Delta t = 2^{-k}\Delta$, with $k = 0, 1, \ldots, 8$ and $\Delta = 0.005$, which are the same as those in Du *et al.* (2018). The benchmark solution for the computing errors is taken as the approximated solution obtained with a smaller time step size $\Delta t = 2^{-8}\Delta/5$. The stabilizing constant is set to be $A = 5$.

Figure 1 plots the discrete ℓ^2 errors of the numerical solutions with various values of ε and δ. The second-order convergence rates are obvious in each case. In comparison with the corresponding results presented in Du *et al.* (2018), we find the numerical errors generated by the BDF2 scheme are less sensitive to the value of δ, especially for large ε, than the ones computed by the Crank–Nicolson version.
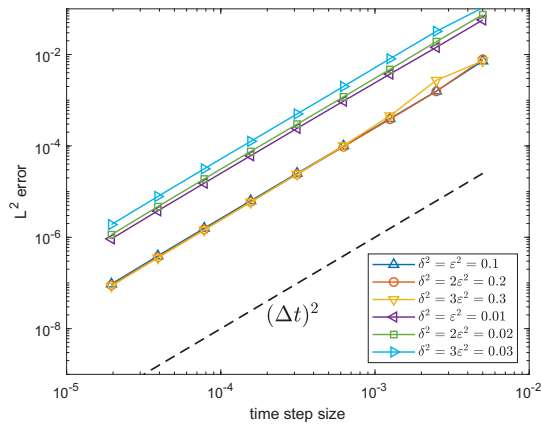
FIG. 1. Temporal convergence rates in Example 4.1.

TABLE 1   *Coefficients of the linear fitting* $E(t) \sim b_e t^{m_e}$ *for the case* $\delta = 0.05$

ε	0.1	0.09	0.08	0.07	0.06	0.05	0.04
m_e	-0.326	-0.314	-0.331	-0.321	-0.327	-0.341	-0.332
b_e	22.763	21.511	19.737	18.312	16.240	14.214	12.365

4.2 *Coarsening dynamics*

It is known (Dai & Du, 2016) that the energy corresponding to the classic Cahn–Hilliard equation satisfies the $-\frac{1}{3}$ power law for the rate of decay, that is, $E(t) \sim t^{-\frac{1}{3}}$ for large t, while there is no similar theoretical result for the NCH equation (1.3). In the following experiment, we will simulate the power law for the NCH equation (1.3) numerically. In fact, the constraints on the time step size declared in the theoretical results are sufficientm but not necessary, and a moderately larger time step will not lead to the violation of the energy stability in practical computations. Thus, to accelerate the simulation of the power law, we will use variable time step sizes in the following experiment without sacrificing the numerical accuracy, as done by Chen *et al.* (2014) and Ju *et al.* (2018).

EXAMPLE 4.2   Setting $\Omega = (-2\pi, 2\pi) \times (-2\pi, 2\pi)$, we simulate the coarsening dynamics of phase transition process with various values of ε and δ shown later. The initial configuration is set to be a random initial data ranging uniformly in $[-0.1, 0.1]$ on each grid point in a uniform mesh. The time step size is set as: $\Delta t = 0.001$ on the time interval $[0, 1000)$, $\Delta t = 0.01$ on $[1000, 10000)$ and $\Delta t = 0.1$ for $t \geqslant 10000$ if needed. The stabilizing constant is given by $A = 5$.

First, we choose $\delta = 0.05$ and $N = 512$, and set ε decreasing from 0.1 to 0.04. Figure 2 displays the evolution of the computed solutions at $t = 1, 3, 10, 100, 400$ and 5000 for the case $\varepsilon = 0.04$. It is obviously observed that the dynamic evolves from the initial disorder state to the ordered states rapidly and then reaches the steady state around $t = 5000$. Figure 3 (left) presents of the energy evolution curves for $\varepsilon = 0.1, 0.08, 0.06$ and 0.04. In comparison with the reference line corresponding to $Ct^{-\frac{1}{3}}$, it can be observed that the rates of energy decay comply with the $-\frac{1}{3}$ power law well for all cases. Table 1 presents the digits of the coefficients of the linear fitting of the energy in the form $E(t) \sim b_e t^{m_e}$. In fact,
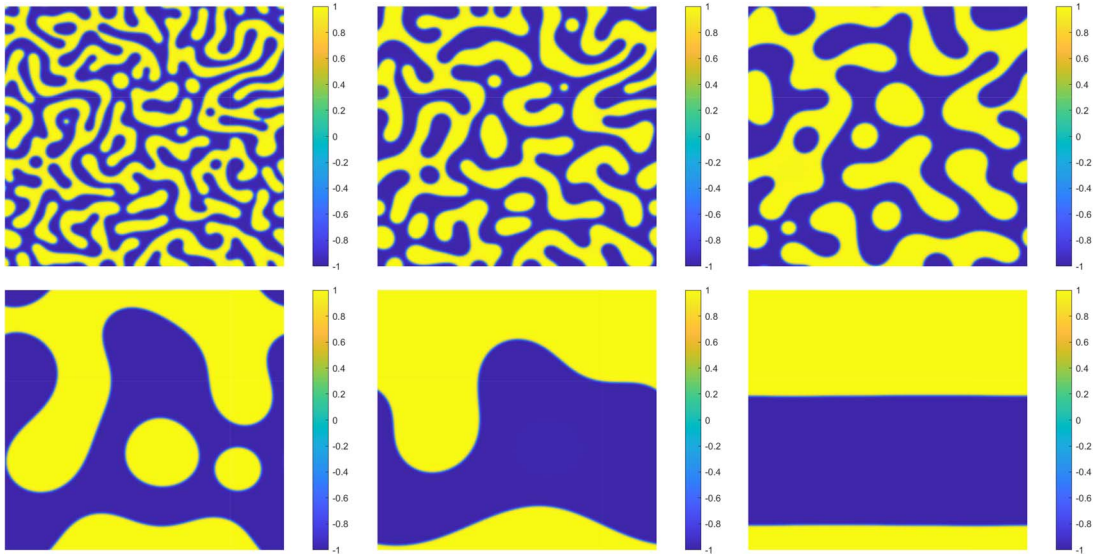
FIG. 2. Computed solutions at $t = 1, 3, 10, 100, 400$ and 5000 for the case $\delta = 0.05$ and $\varepsilon = 0.04$ in Example 4.2.
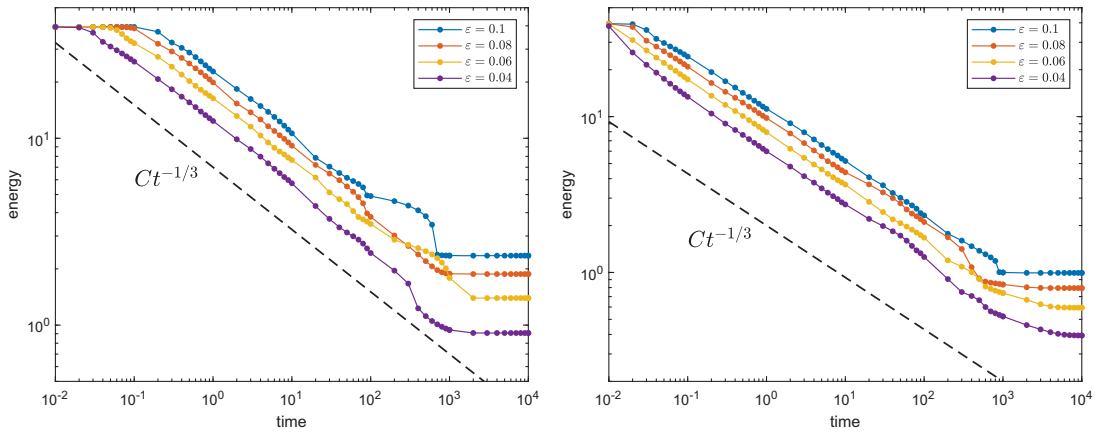

FIG. 3. Evolutions of the energies for case $\delta = 0.05$ (left) and $\delta = 0.005$ (right) in Example 4.2.

this scaling function is nonlinear, while the linear fitting is applied to $\ln(E(t))$, in terms of $\ln t$. All the values of m_e approach to $-\frac{1}{3}$, which also implies the expected power law.

Then, we set $\delta = 0.005$ and $N = 1024$, and still let ε decrease from 0.1 to 0.04. Paralleled to the first case, Fig. 3 (right) and Table 2 show the evolution curves and the coefficients of the fitting of the energies, respectively. Again, the $-\frac{1}{3}$ power law of the energy decay rate is verified.

TABLE 2   *Coefficients of the linear fitting $E(t) \sim b_e t^{m_e}$ for the case $\delta = 0.005$*

ε	0.1	0.09	0.08	0.07	0.06	0.05	0.04
m_e	-0.334	-0.324	-0.341	-0.337	-0.334	-0.344	-0.343
b_e	11.274	10.604	9.675	8.821	7.938	6.943	6.020

5. Conclusion

In this paper, we study a second-order (in time) stabilized BDF-type numerical scheme for the NCH equation, where the Fourier spectral collocation method is adopted for the spatial approximation. The main theoretical results consist of the convergence analysis, by performing a high order consistency analysis, combined with rough error estimate and refined error estimate. In turn, a modified energy stability becomes available. In comparison with a previous work (Li *et al.*, 2021), we apply the second-order convergence estimate to recover an ℓ^∞ bound of the numerical solution, i.e., the numerical solution can be regarded as a small perturbation of the exact solution. The crucial different technique used for the error estimate is that we use $(-\Delta_N)^{-1}(\hat{e}^{n+1} - \hat{e}^n)$ as the test function, rather than the standard form $(-\Delta_N)^{-1}\hat{e}^{n+1}$, for the error equation, so that a higher order temporal truncation error is provided to match the BDF2 discretization.

The spectral accuracy order in the spatial discretization, as indicated by the estimate (3.3), has greatly facilitated the convergence analysis, provided that m is large enough. Of course, one can also adopt the finite difference or other local approaches of spatial discretization. Due to the periodic boundary condition, the matrix for the discrete Laplacian is circulant, and the product of such a circulant matrix and a vector can also be implemented by the fast Fourier transform. In other words, the evaluation of the discrete Laplacian in the central difference method has more or less the same computational cost as the spectral method. However, the central difference yields a truncation error of order $O(h^2)$, which is not high enough to ensure the ℓ^∞ bound of the discrete temporal derivative, i.e., (3.18) with only $m = 2$. To overcome this difficulty, one needs to conduct a higher order asymptotic analysis to supplement the consistency order in both time and space, by constructing a correction field with the truncation error of order $O(\Delta t^3 + h^4)$. This technique is similar to the analysis presented in Section 3.1; also see related works Guan *et al.* (2017, 2014a,b).

Another natural way to develop the second-order numerical schemes is to consider the Crank–Nicolson approximation combined with an appropriate extrapolation for the nonlinear term. However, whether the second-order stabilized linear scheme proposed in Du *et al.* (2018) can be proved to be energy stable with respect to a modified energy is still an open question, which will be our future work.

REFERENCES

BASKARAN, A., LOWENGRUB, J., WANG, C. & WISE, S. (2013) Convergence analysis of a second order convex splitting scheme for the modified phase field crystal equation. *SIAM J. Numer. Anal.*, **51**, 2851–2873.

BATES, P. (2006) On some nonlocal evolution equations arising in materials science. *Nonlinear Dynamics and Evolution Equations* (H. Brunner, X.-Q. Zhao & X. Zou eds). Volume 48 of Fields Institute Communications. Providence, RI, USA: American Mathematical Society, pp. 13–52.

BATES, P., BROWN, S. & HAN, J. (2009) Numerical analysis for a nonlocal Allen-Cahn equation. *Int. J. Numer. Anal. Model.*, **6**, 33–49.

BATES, P. & HAN, J. (2005a) The Dirichlet boundary problem for a nonlocal Cahn-Hilliard equation. *J. Math. Anal. Appl.*, **311**, 289.

BATES, P. & HAN, J. (2005b) The Neumann boundary problem for a nonlocal Cahn-Hilliard equation. *J. Diff. Eqs.*, **212**, 235–277.

BATES, P., HAN, J. & ZHAO, G. (2006) On a nonlocal phase-field system. *Nonlinear Anal. Theory Methods Appl.*, **64**, 2251–2278.

CAHN, J. & HILLIARD, J. (1958) Free energy of a nonuniform system. I. Interfacial free energy. *J. Chem. Phys.*, **28**, 258–267.

CHEN, W., WANG, C., WANG, X. & WISE, S. (2014) A linear iteration algorithm for energy stable second order scheme for a thin film model without slope selection. *J. Sci. Comput.*, **59**, 574–601.

CHENG, K., WANG, C., WISE, S. & YUE, X. (2016) A second-order, weakly energy-stable pseudo-spectral scheme for the Cahn-Hilliard equation and its solution by the homogeneous linear iteration method. *J. Sci. Comput.*, **69**, 1083–1114.

DAI, S. & DU, Q. (2016) Computational studies of coarsening rates for the Cahn-Hilliard equation with phase-dependent diffusion mobility. *J. Comput. Phys.*, **310**, 85–108.

DU, Q., JU, L., LI, X. & QIAO, Z. (2018) Stabilized linear semi-implicit schemes for the nonlocal Cahn-Hilliard equation. *J. Comput. Phys.*, **363**, 39–54.

DU, Q., JU, L., LI, X. & QIAO, Z. (2019a) Maximum principle preserving exponential time differencing schemes for the nonlocal Allen-Cahn equation. *SIAM J. Numer. Anal.*, **57**, 876–898.

DU, Q., TAO, Y., TIAN, X. & YANG, J. (2019b) Asymptotically compatible discretization of multidimensional nonlocal diffusion models and approximation of nonlocal Green's functions. *IMA J. Numer. Anal.*, **39**, 607–625.

DU, Q., JU, L., LI, X. & QIAO, Z. (2021) Maximum bound principles for a class of semilinear parabolic equations and exponential time-differencing schemes. *SIAM Rev.*, **63**, 317–359.

DUAN, C., CHEN, W., LIU, C., WANG, C. & ZHOU, S. (2021) Convergence analysis of structure-preserving numerical methods for nonlinear Fokker-Planck equations with nonlocal interactions. *Math. Meth. App. Sci.* Accepted and published online. https://doi.org/10.1002/mma.8015.

DUAN, C., LIU, C., WANG, C. & YUE, X. (2020) Convergence analysis of a numerical scheme for the porous medium equation by an energetic variational approach. *Numer. Math. Theor. Meth. Appl.*, **13**, 1–18.

E, W. & LIU, J.-G. (1995) Projection method. I: Convergence and numerical boundary layers. *SIAM J. Numer. Anal.*, **32**, 1017–1057.

FIFE, P. (2003) Some nonclassical trends in parabolic and parabolic-like evolutions. *Trends in Nonlinear Analysis, chapter 3* (M. Kirkilionis, S. Kromker, R. Rannacher & F. Tomi eds). Berlin, Heidelberg: Springer, pp. 153–191.

GOTTLIEB, S., TONE, F., WANG, C., WANG, X. & WIROSOETISNO, D. (2012) Long time stability of a classical efficient scheme for two dimensional Navier-Stokes equations. *SIAM J. Numer. Anal.*, **50**, 126–150.

GOTTLIEB, S. & WANG, C. (2012) Stability and convergence analysis of fully discrete Fourier collocation spectral method for 3-D viscous Burgers' equation. *J. Sci. Comput.*, **53**, 102–128.

GUAN, Z., LOWENGRUB, J. & WANG, C. (2017) Convergence analysis for second order accurate schemes for the periodic nonlocal Allen-Cahn and Cahn-Hilliard equations. *Math. Methods Appl. Sci.*, **40**, 6836–6863.

GUAN, Z., LOWENGRUB, J., WANG, C. & WISE, S. (2014a) Second-order convex splitting schemes for nonlocal Cahn-Hilliard and Allen-Cahn equations. *J. Comput. Phys.*, **277**, 48–71.

GUAN, Z., WANG, C. & WISE, S. (2014b) A convergent convex splitting scheme for the periodic nonlocal Cahn-Hilliard equation. *Numer. Math.*, **128**, 377–406.

GUO, J., WANG, C., WISE, S. & YUE, X. (2016) An H^2 convergence of a second-order convex-splitting, finite difference scheme for the three-dimensional Cahn-Hilliard equation. *Commun. Math. Sci.*, **14**, 489–515.

GUO, J., WANG, C., WISE, S. & YUE, X. (2021) An improved error analysis for a second-order numerical scheme for the Cahn-Hilliard equation. *J. Comput. Appl. Math.*, **388**, 113300.

JU, L., LI, X., QIAO, Z. & ZHANG, H. (2018) Energy stability and error estimates of exponential time differencing schemes for the epitaxial growth model without slope selection. *Math. Comp.*, **87**, 1859–1885.

LI, D. & QIAO, Z. (2017a) On second order semi-implicit Fourier spectral methods for 2D Cahn-Hilliard equations. *J. Sci. Comput.*, **70**, 301–341.

LI, D. & QIAO, Z. (2017b) On the stabilization size of semi-implicit Fourier-spectral methods for 3D Cahn-Hilliard equations. *Commun. Math. Sci.*, **15**, 1489–1506.

LI, D., QIAO, Z. & TANG, T. (2016) Characterizing the stabilization size for semi-implicit Fourier-spectral method to phase field equations. *SIAM J. Numer. Anal.*, **54**, 1653–1681.

LI, X., QIAO, Z. & WANG, C. (2021) Convergence analysis for a stabilized linear semi-implicit numerical scheme for the nonlocal Cahn-Hilliard equation. *Math. Comp.*, **90**, 171–188.

LIU, C., WANG, C., WISE, S., YUE, X. & ZHOU, S. (2021) A positivity-preserving, energy stable and convergent numerical scheme for the Poisson-Nernst-Planck system. *Math. Comp.*, **90**, 2071–2106.

SAMELSON, R., TEMAM, R., WANG, C. & WANG, S. (2003) Surface pressure Poisson equation formulation of the primitive equations: Numerical schemes. *SIAM J. Numer. Anal.*, **41**, 1163–1194.

TEMAM, R. (2001) Navier-Stokes equations. *Theory and Numerical Analysis*. Providence, Rhode Island: American Mathematical Society.

TIAN, X. & DU, Q. (2014) Asymptotically compatible schemes for robust discretization of nonlocal models and their local limits. *SIAM J. Numer. Anal.*, **52**, 1641–1665.

WANG, C., LIU, J.-G. & JOHNSTON, H. (2004) Analysis of a fourth order finite difference method for incompressible Boussinesq equations. *Numer. Math.*, **97**, 555–594.

WANG, L., CHEN, W. & WANG, C. (2015) An energy-conserving second order numerical scheme for nonlinear hyperbolic equation with an exponential nonlinear term. *J. Comput. Appl. Math.*, **280**, 347–366.

ZHOU, K. & DU, Q. (2010) Mathematical and numerical analysis of linear peridynamic models with nonlocal boundary conditions. *SIAM J. Numer. Anal.*, **48**, 1759–1780.